Since January 2020 Elsevier has created a COVID-19 resource centre with free information in English and Mandarin on the novel coronavirus COVID-19. The COVID-19 resource centre is hosted on Elsevier Connect, the company's public news and information website.

Journal of Molecular Structure 1224 (2021) 129178

Contents lists available at ScienceDirect

Journal of Molecular Structure

journal homepage: www.elsevier.com/locate/molstr

Exploration of inhibitory action of Azo imidazole derivatives against COVID-19 main protease (M^{pro}): A computational study

Abhijit Chhetri[a], Sailesh Chettri[b], Pranesh Rai[c], Biswajit Sinha[c], Dhiraj Brahman[b,*]

[a] Department of Microbiology, St. Joseph's College, Darjeeling, 734104, India
[b] Department of Chemistry, St. Joseph's College, Darjeeling, 734104, India
[c] Department of Chemistry, University of North Bengal, Darjeeling, 734013, India

ARTICLE INFO

Article history:
Received 1 July 2020
Revised 29 August 2020
Accepted 30 August 2020
Available online 31 August 2020

Keywords:
Azo imidazole
Molecular docking
Binding energy
SARS-CoV-2 M^{pro}
Pharmacokinetics
Remdesivir
Chloroquin
Hydroxychloroquin

ABSTRACT

Four novel ionic liquid tagged azo-azomethine derivatives (L1-L4) have been prepared by the condensation reaction of azo-coupled ortho-vaniline precursor with amino functionalised imidazole derivative and the synthesized derivatives (L1-L4) have been characterized by different analytical and spectroscopic techniques. Molecular docking studies were carried out to ascertain the inhibitory action of studied ligands (L1-L4) against the Main Protease (6LU7) of novel coronavisrus (COVID-19). The result of the docking of L1-L4 showed a significant inhibitory action against the Main protease (M^{pro}) of SARS-CoV-2 and the binding energy (ΔG) values of the ligands (L1-L4) against the protein 6LU7 have found to be −7.7 Kcal/mole (L1), −7.0 Kcal/mole (L2), −7.9 Kcal/mole (L3), and −7.9 Kcal/mole (L4).The efficiency of the ligands has been compared with the FDA approved and clinically trial drugs such as remdesivir, Chloroquin and Hydroxychloroquin and native ligand N3 of main protease 6LU7 to ascertain the inhibitory potential of the studied ligands (L1-L4) against the protein 6LU7. Pharmacokinetic properties (ADME) of the ligands (L1-L4) have also been studied.

1. Introduction

After the outbreak of severe acute respiratory syndrome coronavirus 2 (SARS-CoV-2) in December 2019 from the Wuhan city of China, the infectious disease was declared pandemic by World Health Organization (WHO) on 11the March 2020 and subsequently, the whole world witnessed a global health emergency [1]. As of June 11th 2020, the COVID-19 disease has spread to the whole world with over 7.4 million confirmed cases and over 0.4 million confirmed deaths (worldometer, June 11th 2020). After the declaration of novel coronavirus (COVID-19) infection as pandemic, a number of countries took a preventive measure to slow down the spread of the coronavirus (COVID-19) by implementing mandatory lockdown or national quarantine and as a result of mandatory home quarantine or isolations, more than a third of the planet's population faced some form of restriction (Business Insider, April 17th 2020). Early research on COVID-19 have shown that the cross species and human to human transmission of the virus is regulated by spike protein receptor binding domain and its host receptor (ACE2) as similar to SARS-CoV which was outbreak in 2002 [2]. Till date, no specific vaccine or therapeutic agents are available for the treatment of COVID-19 infection and several existing FDA approved antmaliarial and antiviral drugs have been formulated as a supportive care for the treatment of this infection [3]. Therefore, a rapid formulation of novel compounds as a potentential therapeutic agent for COVID-19 infection is an important mission [4]. Recent studies on SARS-CoV-2 have shown that the 3CL hydrolase (chymotrypsin-like protease, PDB ID: 6LU7), also known as the main protease (Mpro) of novel coronavirus (SARS-CoV-2) plays an important role in the life cycle of coronavirus and thus, its inhibition could provide a promising therapeutic principle for developing strategic and specific treatment against COVID-19 infection [5,6]. Apart from the existing FDA approved antiviral and antimalarial drugs, Traditional Chinese Medicine has gained a lot of interest to treat coronavirus (COVID-19) infection in China [7–12]. Identification of potential inhibitors for specific disease by traditional methods are time consuming and expensive. However, in-silico techniques such as molecular docking and molecular dynamic have gained lot of interest for the identification of potential inhibitors for specific disease in recent years [13,14]. Since, the main protease ($3CL^{pro}$) of coronaviruses is conserved and therefore many research groups are engaged in finding the effective inhibitors for COVID-19 Protease (Mpro) by virtual screening approach using the library of small molecules (antiviral, antimalar-

* Corresponding author. Department of Chemistry, St. Joseph's College, Darjeeling, 734104, India
E-mail address: dhirajslg2@gmail.com (D. Brahman).

https://doi.org/10.1016/j.molstruc.2020.129178
0022-2860/

ial, plant derived, fungal metabolites and synthesized molecules) [15–31]. Recently, computer aided drug design namely molecular docking and molecular dynamic study have gained a lot of interest in the field of drug designing for the treatment of specific disease [32,33]. On the other hand, azo or diazene compounds containing conjugated chromophoric azo (-*N* = *N*-) group are an important class of organic colorants which are mostly studied during recent years [34]. These colorant compounds are widely used as a class of dyes due to their versatile application in various fields such as the dyeing of textile fiber, coloring of different materials, plastics, cosmetics industries, biological-medical studies and advanced application in organic synthesis [35,36]. Furthermore, the azo compounds were found to possess a variety of biological activities such as antibacterial, antifungal, antiviral and anti-inflammatory etc., [37–40]. Interestingly, azo compounds are found to involve in many biological processes such as nitrogen fixation, inhibition of DNA, RNA and protein synthesis, and carcinogenesis [41]. Moreover, Microorganisms, fungi, fungal endophytes, lichenized, ascomycetes, plant parts (bark, berries, leaves, roots, and wood), and marine invertebrates are found to posses natural diazine or azo alkaloids. In recent years, several azo metabolites have been isolated from actenomycetes, fungal species, terrestrial and marine sources [42]. Valanimycin and its derivatives (isloalted from *Streptomyces viridifaciens,* MG456-hF10), maniwamycins A and B (isolated from *Streptomyces prasinopilosus*), azoxybacilin (isolated from *Bacillus cereus,* NR2991), Elaiomycin (isolated from *Streptomyces hepaticus*), Elaiomycins K, L and amide elaiomycin K (isolated from *Streptomyces* sp., Tu¨ 6399), jietacins A and B (isolated from *Streptomyces* sp.), lyophyllin (isolated from mushroom *Lyophyllum shimeji*), calvatic acid (isolated from fungi *Calvatia craniformis*) etc., are the actenomycetes and fungal metabolites which have naturally occurring azo groups and they are found to posses antibiotic activities [43–52]. Thus, it was thought worthwhile to investigate the inhibitory potential of the synthesized azo derivatives against the main protease of COVID-19 and therefore, in this article, we report the computational study on inhibitory action of synthesized Azo imidazole derivatives (L1-L4) against COVID-19 main Protease (M^{pro}).

2. Experimental

2.1. Materials and methods

All the reagents used were of analytical grade and used without further purification. orthovaniline, Aniline, 2 chloroaninline, 4-chloroaniline, and 4-fluoro aniline were procured from Sd fine chemical company, India.1-methylimidazole, KPF_6 and 2-bromoethylaminehydrobromide were procured from sigma Aldrich and used without further purification. All the solvents used were of spectroscopic grade.

2.2. Instrumentation

The IR spectra of the synthesized compounds were analyzed using Perkin-Elmer Spectrum FT-IR spectrometer (RX-1) operating in the region 4000 to 400 cm^{-1} in KBr. ^1H NMR spectra were recorded at room temperature on a FT-NMR (Bruker Advance-II 400 MHz) spectrometer using DMSO–d_6 as solvents and chemical shifts are quoted in ppm downfield of internal standard tetramethylsilane (TMS). Elemental microanalyses (C, H and N) were conducted by using Perkin–Elmer (Model 240C) analyzer. The purity of the prepared compounds was confirmed by thin layer chromatography (TLC) on silica gel plates and the plates were visualized with UV-light and iodine as and when required.

2.3. Preparation of protein and ligand for docking study

The X-ray crystallographic structures of main protease (Mpor, PDB ID 6LU7) of SARS-CoV-2 has been retrieved from the Protein Data Bank (PDB) (http://www.pdb.org.) database. Graphical User Interface program "Auto Dock Tools (ADT) 1.5.6″ from Molecular Graphics Laboratory (MGL) developed by Scripps Research Institute has been employed for the preparation of protein for docking study [53]. Input file of receptor protein for the docking study is created by taking specific china (Chain A) of the protein (6LU7). In a typical receptor protein preparation, water molecules and hetero atoms along with the co-crystallised ligands in PDB crystal structures were removed and subsequently, the receptor .pdbqt file has been created by adding polar hydrogen atoms and Kollman united atom charges [54]. The three dimensional (3D) structures of ligands (L1-L4) were drawn using Chemsketch (ACD/Structure Elucidator, version 12.01, Advanced Chemistry Development, Inc., Toronto, Canada, 2014, http://www.acdlabs.com.) and geometry optimization of the ligands (L1-L4) were carried out using MM2 program incorporated in Chem. Draw Ultra 8.0 and further optimization of geometry of each molecule were carried out with the MOPAC 6 package using the semi-empirical AM1 Hamiltonian [55]. The input .pdbqt file of the ligands was generated using Auto Dock Tools (ADT). As the ligand molecules (L1-L4) are non peptides, therefore, Gasteiger charge was assigned and then non-polar hydrogen was merged. The structure of the ligands L1-L4 is given in Fig. 1.

2.4. Docking study using AutoDock Vina

All molecular docking simulations were carried out in the AutoDock Vina programe 1.1.2 developed by Scripps Research institute [56]. and the results of the docking study and the intermolecular interactions between receptors and the ligand molecules were analyzed using BIOVIA Discovery Studio 2020 (DS), version 20.1.0.0 (Dassault Systèmes BIOVIA, Discovery Studio Modeling Environment, Release 2017, San Diego: Dassault Systèmes, 2016) and Edu pymol version 1.7.4.4 [57]. The three dimensional (3D) affinity (grid) maps and electrostatic a grid boxes of 50×50×50 Å grid points and grid center (X, Y, Z) of −26.283 12.599 58.966 with a spacing of 1.00 Å generated by AutoGrid auxiliary program for each of the receptor for blind docking were generated to cover the entire active site of the receptor protein in order to eliminate any biasness arising during the docking simulation [58]. Lamarckian genetic algorithm and a standard protocol with default setting of other run parameters were used for docking simulation. For each docking experiments, several runs were performed by the program with one predicted binding mode with each run. All the torsions were allowed to rotate. The predicted inhibitory constant (**pK_i**) has been calculated using the following standardized equations [59–61].

$$pK_{i=10^{[\text{Binding Energy Score}/1.336]}}$$

2.5. Synthesis

2.5.1. General procedure for the synthesis of azo imidazole derivatives, L1-L4

azo imidazole derivatives has been synthesized by following the literature procedure given elsewhere [37,62–65]. In a typical synthetic procedure 1-(2-Aminoethyl)−3-methylimidazolium hexafluoro-phosphate, ([2aemim] [PF_6]) (5 mmol) in absolute ethanol was pour in a stirring solution of azo-coupled o-vaniline precursors (5 mmol) in 20 ml of absolute ethanol during a period of 10 min. The reaction mixture was then refluxed in an oil bath for 6 h at 90 °C with constant stirring with the help of magnetic stirrer and the progress of the reaction monitored by TLC

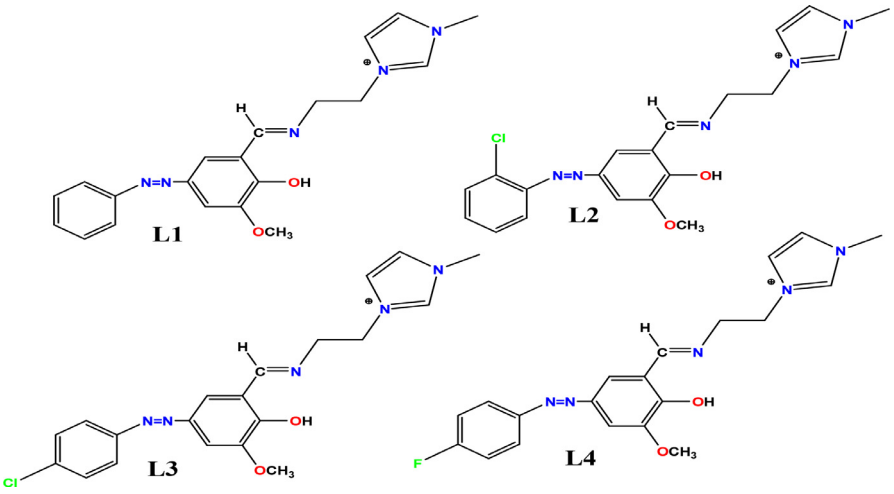

Fig. 1. Structure of Azo Imidazole ligands (L1-L4).

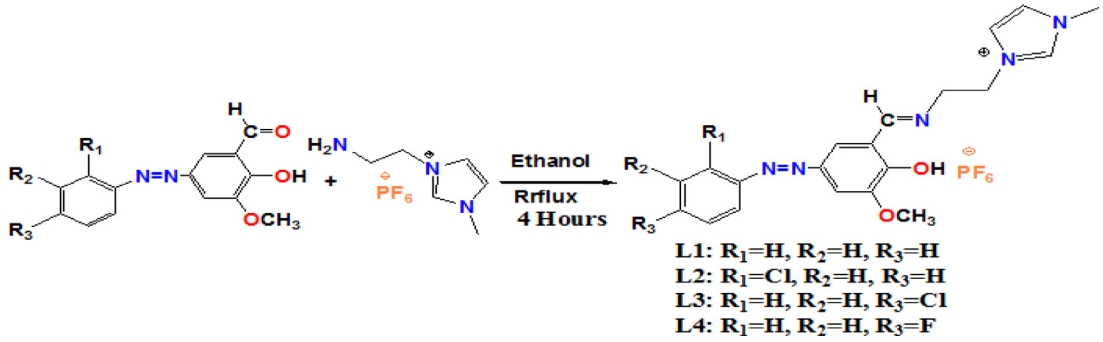

Scheme 1. Syntheses of Azo Imidazole derivatives L1-L4.

(10% ethyl acetate in hexane as eluent). The solution was cooled to room temperature and the solid product thus obtained was filtered, washed with little ethanol and diethyl ether respectively and finally recrystallized from hot ethanol solution and dried over silica under vacuum to get the pure products (Scheme 1).

The analytical and spectroscopic data for each of the synthesized azo imidazole derivatives (L1-L4) are given in supplementary data file SD1.

3. Results and discussion

Azo imidazole derivatives has been successfully prepared by the condensation reaction of 1-(2-Aminoethyl)−3-methylimidazolium hexafluoro-phosphate, ([2aemim] [PF_6]) with substituted azo-coupled o-vaniline precursors in ethanol. All the isolated compounds (L1-L4) were found to be air stable solid, soluble in common organic solvents like methanol, ethanol, acetonitrile, DMF, DMSO etc., and intensely colored compounds.

3.1. IR spectral studies

In order to ascertain the binding mode in the synthesized azo imidazole derivatives L1-L4, the IR spectra of the compounds were closely analyzed. In the solid state IR spectrum of the Azo imidazole derivatives (L1-L4), appearance of bands in the IR spectra of L1-L4 in the range 1620–1647 cm^{-1} can be assigned to the stretching vibration of azomethine linkage ν(-C = N) [64,66]. A strong band at 33,100–3436 cm^{-1} can be assigned to stretching frequency of OH group, ν(OH) group [67]. A band appearing in the range 1593–1616 cm-1 in the IR spectra of L1-L4 derivatives can be assigned to $\nu(C = C)$ stretching frequency. Also, the $N = N$ stretching frequency of the synthesized compounds are found at 1542–1552 cm^{-1} and 1453–1500 cm^{-1} and the $N = N$ bending vibrations are found in the range 1153–1176 cm^{-1} and 956–969 cm^{-1}. IR spectra of the representative compound L1 is depicted in Fig. 2. A band in the range 838–842 cm^{-1} in the IR spectrum of derivatives (L1-L4) can be assigned for stretching vibration of PF_6 group [65]. Thus the IR spectral data therefore supports the formation of the compounds (L1-L4). The IR spectra of L2, L3 and L4 are depicted in supplementary figures (Fig. S1.1-Fig. S1.3).

3.2. ^1H NMR spectral studies

The ^1H NMR spectra of the synthesized azo imidazole derivatives L1-L4 recorded in DMSO–d_6 at ambient temperature, displays a group of signals corresponding to the hydrogen of each molecule. In the ^1H NMR spectrum of L1-L4, the signal corresponds to OH proton exhibited a slightly broad singlet peak at δ 13.3–13.50 ppm and the signal for CH=*N* proton of the compounds L1-L4 appeared as a singlet in the range δ 8.56–8.61 ppm. The appearance of the following peaks, triplet in the range δ 7.62–7.68 ppm for (NCH) proton, triplet in the range δ 7.73–7.76 for (NCH) proton and singlet in the range δ 9.11–9.17 ppm for N (H) CN proton respectively is in good agreement with the proposed structure for the synthesized compounds L1-L4. Signals for NCH_3 and OCH_3 protons appeared in the range δ 3.37–3.76 and δ 3.91–3.97 respectively. The aromatic protons of all the synthesized compounds (L1-L4) appeared as multiplate in the range δ 7.31–7.95 ppm. The NMR spectra of representative compound L1is depicted in Fig. 3 and the NMR spectra of other compounds (L3 and L4) are listed in supplementary figures (Fig. S1.4 & Fig. S1.5).

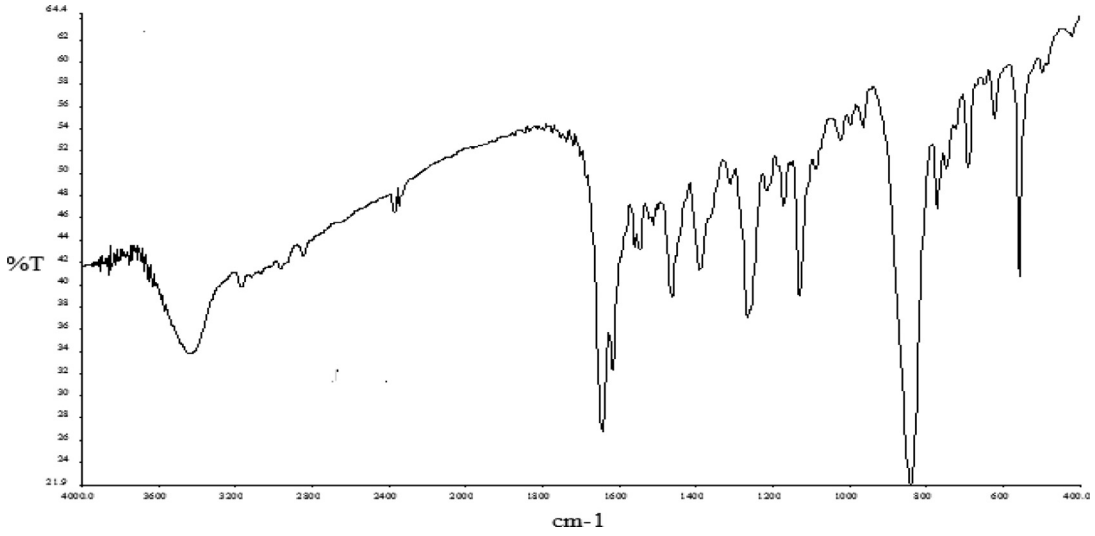

Fig. 2. Infrared Spectra of Compound L1.

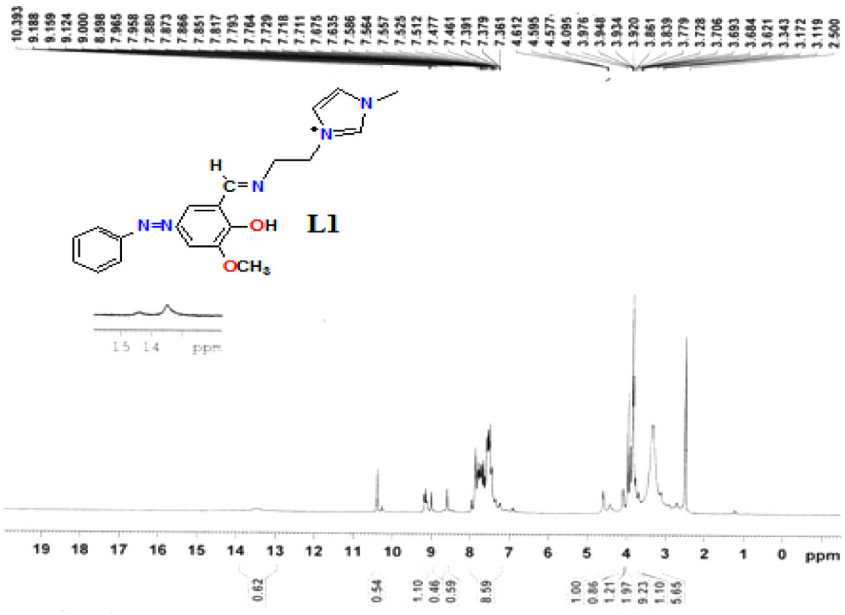

Fig. 3. ^{1}H NMR spectra of compound L1.

3.3. Pharmacokinetic properties of L1-L4

Pharmacokinetics provides information about drug concentrations in the different parts of the organism with respect to time. Drugs when administered into the body of an organism, it needs to cross different biological barriers. Thus, the main properties like absorption, distribution, metabolism and excretion (ADME) are very important parameters for any compounds to be considered as a drug and therefore prior to any clinical and animal studies it is relatively important to ascertain their pharmacokinetic properties of the molecules under consideration [68]. The properties such as lipophilicity (LogPo/W), gastrointestinal absorption (GI), water soluble capability (Log S), and CYP1A2 inhibitor, Blood - Brain Barrier (BBB) are very important pharmacokinetic parameters for any compounds [69]. Therefore, we also determine the pharmacokinetic properties such as lipophilicity (LogPo/W), gastrointestinal absorption (GI), water soluble capability (Log S), and CYP1A2 inhibitor, Blood - Brain Barrier (BBB) of the studied compounds (L1-L4) to ascertain their drug likeness character using SwissADME database (http://www.sib.swiss) and the Lipinski's properties and pharmacokinetic properties of compounds (L1-L4) and standard drug remdesivir are depicted in Table 1 [70].

From Table 1, it is evident that the compounds (L1-L4) with bioavailability 55% have consensus lipophilicity (LogPo/W) value in the range 2.41–2.89. Thus the high and positive lipophilicity values (LogPo/W) which indicates that the compounds are more lipophilic. Lipophilicity is an important phartmacokinetic property of drug candidate in the development of its dosage form, because drug molecules must pass through the lipid bilayer of most cellular membranes. Therefore, generally it is believed that for a drug molecule to have good absorption, it must be lipophilic. According to Lipinski's Rule of Five, the partition coefficient should be positive, but less than 5 i.e., $\log_{10}$PC=5 [71]. Therefore, the studied compounds (L1-L4) with positive and less than 5 (LogPo/W) values can have good absorption in the body and the studied molecules fall on the category of good lipophilic compounds. However, the compounds (L1-L4) are moderately soluble in water as indicated by their solubility (LogS) values which ranges from −3.83 to −4.42. All

Table 1
Lipinski's properties and pharmacokinetic properties (ADME) of the ligands L1-L4 and drug Remdesivir.

Properties	L1	L2	L3	L4	Remdesivir
Molecular weight (gm/mole)	364.42	398.87	398.87	382.41	602.58
Rotatable bonds	7	7	7	7	14
H-bond donor (5)	1	1	1	1	4
H-bond acceptor	5	5	5	6	12
Violations	0	0	0	0	2
Log Po/W	2.41	2.89	2.89	2.70	1.81
Log S	−3.83 (MS)	−4.42 (MS)	−4.42 (MS)	−3.99 (MS)	−4.12 (MS)
GI	High	High	High	High	Low
BBB	No	No	No	No	No
CYP1A2	No	No	No	No	No
Bioavailability Score	0.55	0.55	0.55	0.55	0.17
Topological Surface Area ($Å^2$)	76.40	76.40	76.40	76.40	213.36

*MS: Moderately Soluble, BBB: Blood-Brain Barrier, CYP: Cytochrome P450, GI: Gastrointestinal tract.

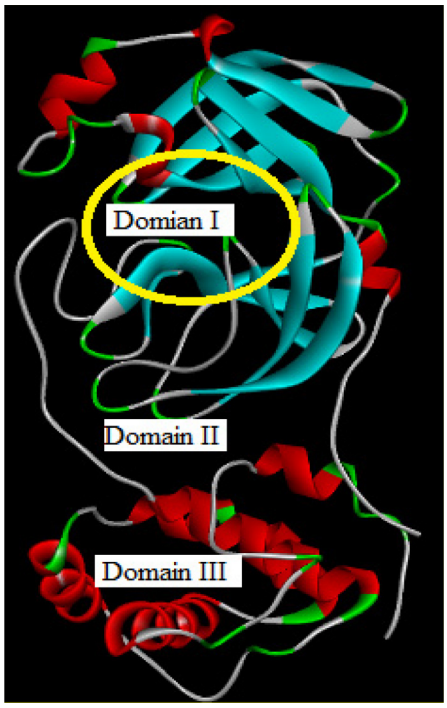

Fig. 4. Structure of M^{pro} of SARS-Cov-2 with domain I, II and III (yellow circle represents catalytically active site).

the studied compounds have high gastrointestinal absorption. The compounds (L1-L4) have no Blood-Brain Barrier and CYP1A2 properties. Thus from the pharmacokinetic analysis, it can be seen that the compounds (L1-L4) qualifies the drug likeness criteria with no Lipinski rule violations and these compounds can serves as a potential drug candidate.

3.4. Molecular docking study

Recent study on structural analysis of M^{pro} of SARS-CoV-2 have shown that it also has same location of active site as Mpro of SARS virus and it is located between the domain I and domain II of protein 6LU7 (Fig. 4).

The catalytic dyad (Cys145-His41) is present on the active site of the protein and both the domain contributes one residue to the catalytic dyad [72,73]. The Cys-His-catalytic dyad of M^{pro} shows protease activity and thus inhibition the catalytic dyad in M^{pro} could become an attractive target for designing anti-CoV drug [74]. As of now, no treapeutic agents or vaccine have been developed specifically to treat the infection caused by SARS-CoV-2 [73]. However, several FDA approved antiviral, anti HIV and anti Malarial drugs have been used as supportive measures to treat and prevent further spread of infection caused by SARS-CoV-2 infection [75–77]. On the other hand, azo containing molecules such as Valanimycin, maniwamycins A and B, Elaiomycin etc., are ubiquitous in nature and these azo compounds are highly bioactive and some of them have been used as antibiotics to cure specific disease [43–45]. Prontosil and Phenazopyridine are FDA approved antibiotic drugs containg Azo group.Prontosil is widely used antibacterial drug which contains azo linkage and sulfonamide group and it has also been used to cure puerperal fever [78,79]. Phenazopyridine is used as local analgesic effects on the urinary tract infection and also sometimes used with antibiotics for immediate symptomatic relief [80]. Since, the traditional method of drug formulation is time consuming and therefore, computational method such as molecular docking and molecular dynamic simulation study may be an alternative way to find out the potential drug candidates for the specific disease at relatively less time [81]. Study of protein- ligand interactions with the help of computer aided drug design method such as molecular docking can provide a promising and potential therapeutic agent for the treatment of specific disease. Therefore, in this study we are utilizing the molecular docking method to study the efficiency of azo imidazole derivatives (L1-L4) as inhibitors of M^{pro} of SARS-CoV-2. The results obtained from these docking studies indicated strong interactions of ligands (L1-L4) with (M^{pro}, 6LU7) of SARS-CoV-2 near the domain pocket I. A summary of the results obtained from successful docking of studied ligands (L1-L4) with main protease (M^{pro}, 6LU7) are summarized in Table 2.

3.5. Visualization of docking results

It has been reported that the amino acid residues His41, Cyd145 and Glu166 are important residues in substrate binding site and involvement of these residues in the formation of hydrogen bond could be prominent for the inhibitory effect of main protease (M^{pro}) [82]. After successful docking of all the ligands (L1-L4) with M^{pro} of SARS-CoV-2, the results showed significant interactions and binding of ligands with the protein 6LU7. The binding energies (ΔG) and predicted inhibitory constant ($\mathbf{pK_i}$) of the ligands (L1-L4) are −7.7 Kcal/mole, −7.0 Kcal/mole, −7.9 Kcal/mole, and −7.9 Kcal/mole respectively and 1.72 μM, 5.76 μM, 1.22 μM and 1.22 μM respectively.

The docking result of L1 with the Protease (6LU7) showed that the ligand (L1) fits inside the core pocket region of the protease at the interface between domain I and domain II (Fig. 5).

A closed analysis of the binding of L1 with the protein 6LU7 revealed that the L1 binds to the protein with binding energy (ΔG)

Table 2
Summary of docking of ligand (L1-L4) against COVID-19 Main Protease (M^{pro}, 6LU7) with their binding energy (ΔG), predicted inhibitory constant (pK_i), interacting amino acid residues and types of interactions.

Ligands	Binding Energy (ΔG) (Kcal/mole)	Predicted inhibitory constant (pK_i) μM	Amino Acid residues	Types of interactions
L1	−7.7	1.72	Gly143 and Ser144 Met165 His163 and His172 Thr24, Thr25, Phe140 and Cys145 Thr26, Leu27, His41, Thr45, Met49, Leu141, Asn142, Glu166 and Gln189	H-bond π-Sulpher π-alkyl π-donor H-bond Van der walls
L2	−7.0	5.76	Leu141, Ser144 and Cys145 His163 and His172 Thr24, Thr26 and Phe140 Thr25, Leu27, His41, Met49, Asn142, Gln143, Met165, Glu166 and Gln189	H-bond π-alkyl π-donor H bond Van der walls
L3	−7.9	1.22	Gly143 and Ser144 Met165 His163 and His172 Thr24, Thr25, Thr26, Phe140 and Cys145 Leu27, His41, Thr45, Met49, Asn142, Glu166, Gln189 and Thr190 Leu141	H-bond π-sulpher π-alkyl π-donor H bond Van der walls Unfavorable Acceptor-acceptor
L4	−7.9	1.22	His41, Leu141 and Cys145 Gln189 and Thr190 His163, Met165 and His172 Thr24, Thr26 and Phe140 Thr25, Leu27, Thr45, Met49, Asn143, Gln143, Ser144 and Glu166	H-bond Halogen (F) bond π-alkyl π-donor H bond Van der walls

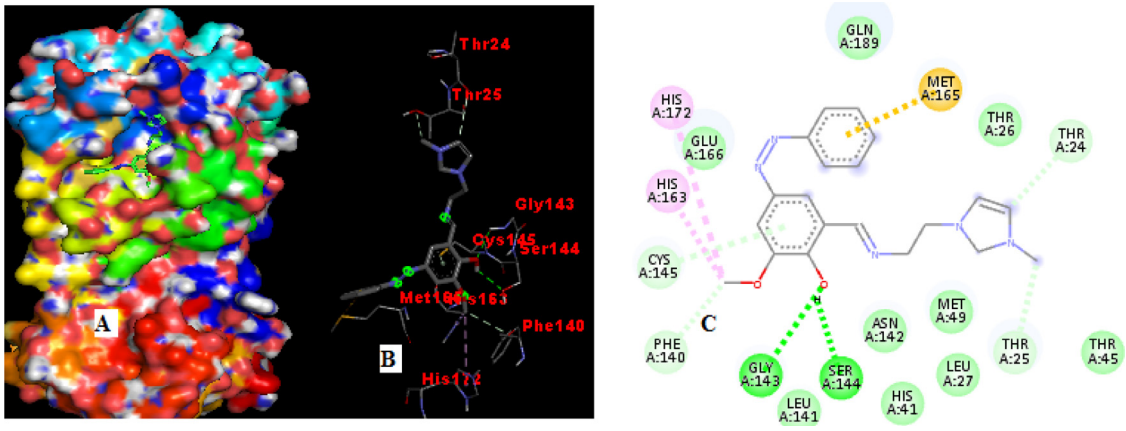

Fig. 5. Visualization of docking of Ligand L1 docked in M^{pro} (6LU7) (A) Best binding mode of protein (Ligand L1 as green and red stick), (B) Amino acid residues involved in hydrogen bonding interaction (green dash line represents H-bonding) and (C) Binding interaction (2D) of ligand L1 with amino acid residues of protein 6LU7 (green dash line represents H-bonding and yellow dashed line represents π-sulpher interaction).

−7.7 Kcal/mole. Ligand L1 forms two hydrogen bonds with protein 6LU7. The first hydrogen bond is formed by NH_2 group of the amino acid residue Gly143 with O atom of OH group of ligand L1 at a distance 2.58 Å and the second hydrogen bond is formed between OH group of residue Ser144 and proton (H) of OH group of ligand L1 at a distance 2.50 Å. Apart from hydrogen bond, S atom of residue Met165 form π-Sulpher bond with π electrons of azobenzene moiety. π-alkyl interactions also exist between the π-electro of residues His163 and His172 and OCH_3 group of L1. The amino acid residues Thr25, Thr25 Cys145 and Phe140 form π-donor hydrogen bonds with L1. The residues ThrR26, Thr45, Leu27, His41, Met49, leu141, Asn142 Glu160 and Gln189 are observed to interact with the ligand L1 through Van der walls interactions.

The visualization of docking result of L2 with main protease (6LU7) revealed that the L2 binds with the Protein at the interface between domain I and domain II with binding energy −7.0 Kcal/mole. It shows significant binding with three hydrogen bonding interactions between, $C = O$ group of amino acid residue Leu141, OH group of residue Ser144 and proton (H) of OH group of L2 at a distance 1.74 Å and 2.88 Å respectively and NH(amide) group of residue Cys145 with O atom of OH group of L2 at a distance 2.59 Å (Fig. S1.6). The other types of interactions are π-alkyl interactions between the π-electron of residues His163 and His172 and OCH_3 group of L2.The residues Thr24, Thr26 and Phe140 are found to interact with the ligand L2 through π-donor hydrogen bond. Apart from these, amino acid residues Thr25, Leu27, His41, Met49, Asn142, Gly143, Met165, Glu166 and Gln189 found to interacts with the ligand L2 through Van der walls interactions.

The docking of ligand L3 with the protein 6LU7 revealed that the ligand binds tightly with the protein residues with binding energy −7.9 Kcal/mole and the significant interactions are characterized by two hydrogen bonds. The first hydrogen bond is formed between the NH_2 group of residue Gly143 and O atom of OH group of L3 at a distance 2.21 Å and second hydrogen bond exist be-

Table 3
Comparison of binding energy (ΔG) of ligand (L1 –L4) with previously reported docking result of some FDA approved and clinically trial antiviral and anti malarial drugs and ligand N3 against main protease of Covid-19 (6LU7).

Compounds (drugs)	Binding energy, ΔG (Kcal/mol)
Remdesvir	−5.8 [83], −7.215 [84], −2.47 [30] −6.5 [85] −9.70 [87]
Chloroquine	−7.5 [83], −3.62 [30] −5.1 [85] −5.75 [86]
Hydroxychloroquine	−6.7 [85] −5.21 [86]
N3	−7.7716 [87], −8.396 [88]
L1	−7.7 [this work]
L2	−7.0 [this work]
L3	−7.9 [this work]
L4	−7.9[this work]

tween the OH group of amino acid residue Ser144 and proton (H) of OH group of L3 at a distance 2.81 Å. The residue Met165 form π-Sulpher interactions between the π-electron of ligand L3 and S atom of amino acid residue (Fig. S1.7). The other types of interactions are π-alkyl (π electron of His163 and His172 with OCH_3 group) and π-donor hydrogen bonds (Thr24, Thr25, Thr26, Phe140 and Cys145). Apart from these interactions, the residues Leu27, His41, Thr45, Met49, Asn142, Glu166, Gln189 and Thr190 are found to interact with L3 through Van der walls interactions. An unfavorable acceptor-acceptor interaction between the ligand and residue Leu141 has also been observed.

The visualization of docking result of ligand L4 with the protein 6LU7 revealed that the ligand binds with the protein residues near the interface of domain I and domain II with binding energy (ΔG) −7.9 Kcal/mole. Three hydrogen bonding interactions exist between the protein residues and ligand L4. The two hydrogen bonds are found to exist at the catalytic dyad (Cys145-His41) between the NH (imidazole ring) of residue His41 and N atom of azomethine ($C = N$) group of ligand at a distance 2.91 Å and NH_2 group of residue Cys145 and O atom of OH group of L4 at a distance 2.65 Å. The other hydrogen bond is formed by the $C = O$ group of residue Leu141 with proton (H) of OH group of L4 at a distance 2.19 Å (Fig. S1.8). The $C = O$ (amide) group of residue Gln189 and $C = O$ group of residue Thr190 have been found to form halogen bond with F atom of L4 at a distance 3.60 Å and 3.56 Å respectively. Other interactions include π-alkyl (π electron of residues His163, Met165 and His172 and OCH_3 group of L4) and π-donor hydrogen bond (Thr24, Thr26 and Phe140). The amino acid residues Thr25, Leu27, Thr45, Met49, Asn142, Glu143, Ser144 and Glu166 found to interact with the ligand through Van der walls interactions.

The binding energy (ΔG) value of ligands L1-L4 has been compared with the previously reported binding energy (ΔG) values of FDA approved and clinically trial antiviral and antimalarial drugs such as Remdesivir, choloroquin and hydroxychloroquine and native ligand N3 of protein 6LU7 in order to ascertain the inhibitory potential of the studied ligands (L1-L4) against the main protease (6LU7) of SARS-CoV-2 and it is represented in Table 3.

Therefore, it is evident from Table 3 that the clinically trial antiviral drug Remdesivir has binding energy (ΔG) in the range −2.47—9.70, antimalarial drugs, Chloroquin and Hydroxychloroquin has binding energy (ΔG) in the range −3.63—7.5 Kcal/mole respectively and the ligand N3 has binding energy (ΔG) value in the range −7.77—8.36 Kcal/mole. In our work the binding energy (ΔG) value of the ligands (L1-L4) have been found to be −7.7 Kcal/mole (L1), −7.0 Kcal/mole (L2), −7.9 Kcal/mole (L3) and 7.9 Kcal/mole (L4) respectively. Thus from this comparison, it may be conclude that the ligands (L1-L4) could act as a potential inhibitor molecule against SARC–CoV-2.

4. Conclusion

In this article, we have reported the molecular docking study of four ligands (L1-L4) against the main protease (6LU7) of SARS-CoV-2 to ascertain the inhibitory potential of these ligands. The docking results attributed various types of protein- ligand interactions and it is also seen that the lignads shows significant interactions at the interface between domain I and domain II. Furthermore, most of the ligands show interaction at the Cys-His-catalytic dyad. The pharmacokinetic study has revealed that the ligands (L1-L4) could act as a potential drug candidate. Thus, it is evident that various kind of favorable interactions exist between the ligands (L1-L4) and the main protease 6LU7. Therefore, on the basis of computational study, it may concluded that the ligands (L1-L4) could act as potential inhibitor against the main protease (6LU7) of SARS-CoV-2. Furthermore, *in vivo* and *in vitro* study is required to ascertain the proper binding mechanism and understanding the drug behavior of the studied ligands (L1-L4).

Declaration of Competing Interest

The authors do not have any conflict of interest.

CRediT authorship contribution statement

Abhijit Chhetri: Conceptualization, Formal analysis, Funding acquisition, Software, Validation, Writing - original draft, Writing - review & editing. **Sailesh Chettri:** Data curation, Formal analysis, Funding acquisition, Investigation, Methodology, Validation, Writing - original draft. **Pranesh Rai:** Investigation, Methodology, Project administration, Validation. **Biswajit Sinha:** Conceptualization, Methodology, Project administration, Supervision, Visualization, Writing - review & editing. **Dhiraj Brahman:** Conceptualization, Data curation, Formal analysis, Funding acquisition, Investigation, Methodology, Project administration, Software, Supervision, Validation, Visualization, Writing - original draft, Writing - review & editing.

Acknowledgements

The authors are grateful to the research facilities available at the Department of Chemistry, University of North Bengal and St. Joseph's College, Darjeeling. All the authors are thankful to Sophisticated Analytical Instrument Facility (SAIF), NEHU, Shilong, India for NMR and elemental analysis.

Supplementary materials

Supplementary material associated with this article can be found, in the online version, at doi:10.1016/j.molstruc.2020.129178.

References

[1] C.R. MacIntyre, Global spread of COVID-19 and pandemic potential, Global Biosecurity 1 (3) (2020), doi:10.31646/gbio.55.
[2] W.H. Li, M.J. Moore, N. Vasilieva, J.H. Sui, S.K. Wong, M.A. Berne, M. Somasundaran, J.L. Sullivan, K. Luzuriaga, T.C. Greenough, H. Choe, M. Farzan, Angiotensin-converting enzyme 2 is a functional receptor for the SARS coronavirus, Nature 426 (2003) 450–454, doi:10.1038/nature02145.
[3] M.L. Sun, J.M. Yang, Y.P. Sun, G.H. Su, Inhibitors of RAS Might Be a Good Choice for the Therapy of COVID-19 Pneumonia, Chin. J. Tuber. Resp. dis. 43 (3) (2020) 219-222, doi:10.3760/cma.j.issn.1001-0939.2020.03.016.
[4] K. Harismah, M. Mirzaei, Favipiravir: structural Analysis and Activity against COVID-19, Adv. J. Chem. Section B 2 (2) (2020) 55–60, doi:10.33945/SAMI/AJCB.2020.2.3.
[5] Z. Jin, X. Du, Y. Xu, Y. Deng, M. Liu, Y. Zhao, B. Zhang, X. Li, L. Zhang, C. Peng, Y. Duan, J. Yu, L. Wang, K. Yang, F. Liu, R. Jiang, X. Yang, T. You, X. Liu, X. Yang, F. Bai, H. Liu, X. Liu, L.W. Guddat, W. Xu, G. Xiao, C. Qin, Z. Shi, H. Jiang, Z. Rao, H. Yang, Structure of M^{pro} from SARS-CoV-2 and discovery of its inhibitors, Nature (2020) 1–24, doi:10.1038/s41586-020-2223-y.

[6] M. Wang, R. Cao, L. Zhang, X. Yang, J. Liu, M. Xu, Z. Shi, Z. Hu, W. Zhong, G. Xiao, Remdesivir and chloroquine effectively inhibit the recently emerged novel coronavirus (2019-nCoV) in vitro, Cell Res 3 (2020) 269-271, doi:10.1038/s41422-020-0282-0.
[7] Y. Yang, M.S. Islam, J. Wang, Y. Li, X. Chen, Traditional Chinese Medicine in the Treatment of Patients Infected with 2019-New Coronavirus (SARS-CoV-2): a Review and Perspective, Inter. Int. J. biol. Sci. 16 (10) (2020) 1708–1717, doi:10.7150/ijbs.45538.
[8] G. Li, E. De Clercq, Therapeutic options for the 2019 novel coronavirus (2019-nCoV), Nat. Rev. Drug Discov. 19 (3) (2020) 149-150, doi:10.1038/d41573-020-00016-0.
[9] J. Xu, Y. Zhang, Traditional Chinese Medicine treatment of COVID-19, Complement. Ther. Clin. Pract. 39 (2020) 1–2, doi:10.1016/j.ctcp.2020.101165.
[10] Ren J-l, Zhang A-H, Wan X-J, Traditional Chinese medicine for COVID-19 treatment, Pharma. Res. 155 (2020) 1–2, doi:10.1016/j.phrs.2020.104743.
[11] Ling C-Q, Traditional Chinese medicine is a resource for drug discovery against 2019 novel coronavirus (SARS-CoV-2), J. Integr. Med. 18 (2) (2020) 87–88, doi:10.1016/j.joim.2020.02.004.
[12] D. Hong-Zhi, H. Xiao-Ying, M. Yu-Huan, H. Bi-Sheng, L. Da-Hui, Traditional Chinese Medicine: an effective treatment for 2019 novel coronavirus pneumonia (NCP), Chin. J. Nat. Med. 18 (3) (2020) 206–210, doi:10.1016/S1875-5364(20)30022-4.
[13] M.T. ul Qamar, A. Maryam, I. Muneer, F. Xing, U.A. Ashfaq, F.A. Khan, F. Anwar, M.H. Geesi, R.R. Khalid, S.A. Rauf, A.R. Siddique, Computational screening of medicinal plant phytochemicals to discover potent pan-serotype inhibitors against dengue virus, Sci. Rep. 9 (1) (2019) 1–16, doi:10.1038/s41598-018-38450-1.
[14] X. Xia, Bioinformatics and Drug Discovery, Curr. Top. Med. Chem. 17 (15) (2017) 1709–1726, doi:10.2174/1568026617666161116143440.
[15] A.D. Sharma, I. Kaur, Jensenone from eucalyptus essential oil as a potential inhibitor of COVID 19 corona virus infection, Res. & Rev. in Biotech. & Biosci. 7 (1) (2020) 59–66, doi:10.5281/zenodo.3748477.
[16] A. Ubani, F, Agwom, N.Y. Shehu, P. Luka, A. Umera, U. Umar, S. Omale, N.E. Nnadi, J.C. Aguiyi, Molecular docking analysis of some phytochemicals on two sars-cov-2 targets. bioRxiv Preprint, (2020), 1–14. doi: 10.1101/2020.03.31.017657.
[17] P. Sang, S.H. Tian, Z.H. Meng, L.Q. Yang, Anti-HIV drug repurposing against SARS-CoV-2, RSC Adv 10 (2020) 15775–15783, doi:10.1039/D0RA01899F.
[18] I. Halifa, W. Zhu, M.S. Nafie, K. Dutta, C. Li, Anti-COVID-19 Effects of Ten Structurally Different Hydrolysable Tannins through Binding with the Catalytic-Closed Sites of COVID-19 Main Protease: an In-Silico Approach, Preprints (2020) 1–21 2020030277, doi:10.20944/preprints202003.0277.v1.
[19] R.R. Narkhede, R.S. Cheke, J.P. Ambhore, S.D. Sindhe, The Molecular Docking Study of Potential Drug Candidates Showing Anti-COVID-19 Activity by Exploring of Therapeutic Targets of SARS-CoV-2, Eur. J. Med. and Oncol. 4 (3) (2020) 185–195, doi:10.14744/ejmo.2020.31503.
[20] M. Hastantram, S. Ramaiah, R. Vishwakarma, R.U. Shaanker, Molecular docking analysis of selected natural products from plants for inhibition of SARS-CoV-2 main protease, Curr. Sci. 118 (7) (2020) 1–6, doi:10.18520/cs/v118/i7/1087-1092.
[21] P. Singh, A. Sharma, S.P. Nandi, Identification of Potent Inhibitors of COVID-19 Main Protease Enzyme by Molecular Docking Study, Chemrxiv (2020) 1–13, doi:10.26434/chemrxiv.12179202.v1.
[22] J. Lung, Y.-.S. Lin, Y.-.H. Yang, Y.-.L. Chou, Ll-H. Shu, Y.-.C. Cheng, H.T. Liu, C.-.Y. Wu, The potential chemical structure of anti-SARS-CoV-2RNA-dependent RNA polymerase, J. Med. Virol. 92 (2020) 693–697, doi:10.1002/jmv.25761.
[23] N. Muralidharan, R. Sakthivel, D. Velmurugan, M.M. Gromiha, Computational studies of drug repurposing and synergism of lopinavir, oseltamivir and ritonavir binding with SARS-CoV-2 protease against COVID-19, J. Biomol. Struct. Dyn. (2020) 1–7, doi:10.1080/07391102.2020.1752802.
[24] D.C. Hall Jr, H.F. Ji, A Search for Medications to Treat COVID-19 via in Silico Molecular Docking Models of the SARS-CoV-2 Spike Glycoprotein and 3CL Protease, Trav. Med. Infect. Dis. (2020) article in press, doi:10.1016/j.tmaid.2020.101646.
[25] O.M. Aly, Molecular Docking Reveals the Potential of Aliskiren, Dipyridamole, Mopidamol, Rosuvastatin, Rolitetracycline and Metamizole to Inhibit COVID-19 Virus Main Protease, ChemRxiv (2020) 1–13, doi:10.26434/chemrxiv.12061302.v1.
[26] S. Pant, M. Singh, V. Ravichandiran, U.S.N. Murty, H.K. Srivastava, Peptide-like and small-molecule inhibitors against Covid-19, J. Biomol. Struct. Dyn. (2020) 2–23 article in press, doi:10.1080/07391102.2020.1757510.
[27] Y.-.C. Chang, Y.-.A. Tung, K.-.H. Lee, T.-.F. Chen, Y.-.C. Hsiao, H.-.C. Chang, T.-.T. Hsieh, C.-.H. Su, S.-.S. Wang, J.-.Y. Yu, S. Shih, Y.-.H. Lin, Y.-.H. Lin, Y.-.C. Ethan Tu, C.-.W. Tung, C.-.Y. Chen, Potential therapeutic agents for COVID-19 based on the analysis of protease and RNA polymerase docking. Preprints, (2020), 1–7. doi: 10.20944/preprints202003.0277.v1.
[28] T. Sekhar, Virtual Screening based prediction of potential drugs for COVID-19. Preprints, (2020), 1–25. doi: 10.20944/preprints202002.0418.v2.
[29] D.L. McKee, A. Sternberg, U. Stange, S. Laufer, C. Naujokat, Candidate Drugs against SARS-CoV-2 and COVID-19, Pharma. Res. 157 (2020) 1–9, doi:10.1016/j.phrs.2020.104859.
[30] M.F. Khan, M.A. Khan, Z.A. Khan, T. Ahamad, W.A. Ansari, Identification of Dietary Molecules as Therapeutic Agents to Combat COVID-19 Using Molecular Docking Studies, Research Square (2020) 1–17 Preprint, doi:10.21203/rs.3.rs-19560/v1.
[31] I. Anouz, A. Belhassan, K. El-Khatabi, T. Lakhlifi, M. El-Ldrissi, M. Bouachrine, Moroccan Medicinal plants as inhibitors against SARS-CoV-2 main protease: computational investigations, J. Biomol. Struct. Dyn. (2020) 1-9, doi:10.1080/07391102.2020.1758790.
[32] W. Yu, A.D. MacKerell Jr, Computer-Aided Drug Design Methods, Methods Mol. Biol. 1520 (2017) 85–106.
[33] B.K.Singh Surabhi, Computer aided drug design: an overview, J. Drug Del. & Ther. 8 (5) (2018) 504–509, doi:10.22270/jddt.v8i5.1894.
[34] E. Ispir, The synthesis, characterization, electrochemical character, catalytic and antimicrobial activity of novel, azo-containing Schiff bases and their metal complexes, Dyes and Pigments 82 (2009) 13–19, doi:10.1016/j.dyepig.2008.09.019.
[35] H. Song, K. Chen, D. Wu, H. Tan, Synthesis and absorption properties of some new azo-metal chelates and their ligands, Dyes and Pigments 60 (2004) 111–119, doi:10.1016/S0143-7208(03)00144-X.
[36] A. Peters, T.E. Chisowa, Colour-constitution relationships in 2-acylamino-4-N,N-diethylaminoazobenzene disperse dyes, Dyes and Pigments 22 (1993) 223–238, doi:10.1016/0143-7208(93)80015-S.
[37] A.A. Jarrahpour, A.R. Esmaeilbeig, M. Zarei, Synthesis of 2-hydroxy-3-methoxy-5-(4-methoxyphenylazo) benzaldehyde. A new aldehyde for the preparation of biologically active molecules, Molbank M371 (1) (2004) 1–2, doi:10.3390/M371.
[38] H. Xu, X. Zeng, Synthesis of diaryl-azo derivatives as potential antifungal agents, Bioorg. & Med. Chem. Letters. 20 (14) (2010) 4193–4195, doi:10.1016/j.bmcl.2010.05.048.
[39] E.M. Flefel, R.E. Abdel-Mageid, W.A. Tantawy, M.A. Ali A-G. Amr, Heterocyclic compounds based on 3-(4-bromophenyl) azo-5-phenyl-2(3H)-furanone: anti-avian influenza virus (H5N1) activity, Acta Pharma 62 (4) (2012) 593-606, doi:10.2478/v10007-012-0037-7.
[40] M. Tonell, I. Vazzana, B. Tasso, V. Boido F. Sparatore, M. Fermeglia, M. SilviaPaneni, P. Posocco, S. Pricl, P. LaColla, C. Ibba, B. Secci, G. Collu, R. Loddo, Antiviral and cytotoxic activities of aminoarylazo compounds and aryltriazene derivatives, Bioorg. & Med. Chem. 17 (13) (2009) 4425–4440, doi:10.1016/j.bmc.2009.05.020.
[41] M. Badea, R. Olar, F. Cristurean, D. Marinescu, A. Emandi, P. Budrueeac, E. Segal, Thermal stability study of some azo-derivatives and their complexes: part 2. New azo-derivative pigments and their Cu (II) complexes, J. Ther. Anal. Calor. 77 (3) (2004) 815–824, doi:10.1023/B:JTAN.0000041660.12310.c7.
[42] V.M. Dembitsky, T.A. Gloriozova, V.V. Poroikov, Pharmacological and Predicted Activities of Natural Azo Compounds, Nat. Prod. Bioprospect. 7 (2017) 151–169, doi:10.1007/s13659-016-0117-3.
[43] M. Yamato, H. Iinuma, H. Naganawa, Y. Yamagishi, M. Hamada, T. Masuda, H. Umezawa, V. Abe, M. Hori, Isolation and properties of valanimycin, a new azoxy antibiotic, J. Antibiot. 39 (2) (1986) 184–191, doi:10.7164/antibiotics.39.184.
[44] Y. Ma, J. Patel, R.J. Parry, A novel valanimycin-resistance determinant (vlmF) from Streptomyces viridifaciens MG456-hF10, Microbiol 146 (Pt 2) (2006) 345-352, doi:10.1099/00221287-146-2-345.
[45] M. Nakayama, Y. Takahashi, H. Itoh, K. Kamiya, M. Shiratsuchi, G. Otani, Novel Antifungal Antibiotics Maniwamycins A and B, J. Antibot. 42 (1989) 1535–1540, doi:10.7164/antibiotics.42.1535.
[46] M. Fujiu, S. Sawairi, H. Shimada, Y.Aoki H.Takaya, T. Okuda, K. Yokose, Azoxybacilin, a Novel Antifungal Agent Produced by Bacillus Cereus NR2991. Production, Isolation and Structure Elucidation, J. Antibiot. 47 (1994) 833–835, doi:10.7164/antibiotics.47.833.
[47] T.H. Haskell, A. Ryder, Q.R. Bartz, Elaiomycin, a new tuberculostatic antibiotic; isolation and chemical characterization, Antibiot. Chemother. (Northfield, Ill.) 4 (2) (1954) 141–144.
[48] S. Omura, K. Otoguro, N. Imamura, H. Kuga, Y. Takahasi, R. Masuma, Y. Tanaka, H. Tanaka, S. Xue-Hui, Y. En-Tai, Jietacins A and B, new nematocidal antibiotics from a streptomyces sp, J. Antibiot. 40 (5) (1987) 623–629, doi:10.7164/antibiotics.40.623.
[49] N. Imamura, H. Kuga, K. Otoguro, H. Tanaka, S. Omura, Structures of Jietacines: unique α, β-unsaturated azoxy antibiotics, J. Antibiot. 42 (1989) 156–158, doi:10.7164/antibiotics.42.156.
[50] K. Tsuzuki, F.S. Yan, K. Otoguro, S. Omura, Synthesis and nematocidal activities of Jietacin A and its analogs, J. Antibiot. 44 (1991) 774–784, doi:10.7164/antibiotics.44.774.
[52] W.Y. Chan, T.B. Ng, J.S. Lam, J.H. Wong, The mushroom ribosome-inactivating protein lyophyllin exerts deleterious effects on mouse embryonic development in vitro, Appl. Microbiol. Biotech. 85 (2010) 985–993, doi:10.1007/s00253-009-2048-y.
[51] H. Umezawa, T. Takeuchi, H. Iinuma, M. Ito, M. Ishizuka, A New Antibiotic, Calvatic Acid, J Antibiot. 28 (1975) 87–90, doi:10.7164/antibiotics.28.87.
[53] R. Huey, G.M. Morris, The Scripps Research Institute, USA (2008), 54–56.
[54] A.M. Vijesh, A.M. Isloor, S. Telkar, T. Arumoli, H.K. Fun, Molecular docking studies of some new imidazole derivatives for antimicrobial properties, Arab. J. Chem. 6 (2013) 197–204, doi:10.1016/j.arabjc.2011.10.007.
[55] K. Ohtawara, H. Teramae, Study on optimization of molecular structure using Hamiltonian algorithm, Chem. Phys. Letters 390 (2004) 84–88, doi:10.1016/j.cplett.2004.03.088.
[56] O. Trott, A.J. Olson, AutoDock Vina: improving the speed and accuracy of docking with a new scoring function, efficient optimization and multithreading, J. Comp. Chem. 31 (2020) 455–461, doi:10.1002/jcc.21334.
[57] W.L. DeLano, Pymol: an open-source molecular graphics tool. CCP4 Newsletter on protein crystallography, 40(1) (2002), 82–92.

[58] G.M. Morris, D.S. Goodsell, R.S. Halliday, R. Huey, W.E. Hart, R.K. Belew, A.J. Olson, Automated docking using a Lamarckian genetic algorithm and an empirical binding free energy function, J. Comp. Chem. 19 (14) (1998) 1639–1662. doi:10.1002/(SICI)1096987X(19981115)19:14<1639::AID-JCC10>3.0.CO;2-B.
[59] A.L. Hopkins, C.R. Groom, A. Alex, Ligand efficiency: a useful metric for lead selection, Drug discov. Today 9 (10) (2004) 430–431, doi:10.1016/S1359-6446(04)03069-7.
[60] M.A. Alamri, M.T. Ul Qamar, M.U. Mirza, R. Bhadane, S.M. Alqahtani, I. Muneer, M. Froeyen, O.M.H. Salo-Ahen, Pharmacoinformatics and molecular dynamics simulation studies reveal potential covalent and FDA-approved inhibitors of SARS-CoV-2 main protease 3CLpro, J. Biomol. Struct. Dyn. (2020) 1–14, doi:10.1080/07391102.2020.1782768.
[61] C.W. Murray, D.A. Erlanson, A.L. Hopkins, G.M. Keserü, P.D. Leeson, D.C. Rees, C.H. Reynolds, N.J. Richmond, Validity of Ligand Efficiency Metrics, ACS Med. Chem. Lett. 5 (6) (2014) 616–618, doi:10.1021/ml500146d.
[62] V.S. Kumar, Y.S. Mary, K. Pradhan, D. Brahman, Y.S. Mary, R. Thomas, M.S. Roxy, C.V. Alsenoy, Synthesis, spectral properties, chemical descriptors and light harvesting studies of a new bioactive azo imidazole compound, J. Mol. Str. 1199 (2020) 1–10 127035, doi:10.1016/j.molstruc.2019.127035.
[63] B. Li, Y.-Q. Li, Y.-P. Caib, M.Y. Zhou, 1-{2-[(2-*hydroxybenzylidene*)-*amino*]-ethyl}-3-methyl-3H-imidazolium hexafluorophosphate, Structure Reports, Acta Cryst. Section E e64 (2008) o2365, doi:10.1107/S1600536808037124.
[64] S. Saha, A. Das, K. Acharjee, B. Sinha, Synthesis, characterization and antibacterial studies of Mn(II) and Co(II) complexes of an ionic liquid tagged Schiff base, J. Serb. Chem. Soc. 81 (10) (2016) 1151–1159, doi:10.2298/JSC160425065S.
[65] B. Li, Y.-Q. Li, W.J. Zheng, M.-Y. Zhou, Synthesis of ionic liquid-supported Schiff bases, ARKIVOC, (xi) (2009), 165–171.
[66] S. Saha, G. Basak, B. Sinha, Physico-chemical characterization and biological studies of newly synthesized metal complexes of an Ionic liquid-supported Schiff base: 1-{2-[(2-hydroxy-5-bromobenzylidene) amino] ethyl}-3- ethylimidazolium tetrafluoroborate, J. Chem. Sci. 30 (9) (2018) 1–9, doi:10.1007/s12039-017-1409-9.
[67] B. Khungar, M.S. Rao, K. Pericherla, P. Nehra, N. Jain, J. Panwar, A. Kumar, Synthesis, characterization and microbiocidal studies of novel ionic liquid tagged Schiff bases, Comp. Ren. Chim. 15 (2012) 669–674, doi:10.1016/j.crci.2012.05.02.
[68] K. Boussery, F.M. Johan, V. De. Voorde, Chapter 31 - Physiological Aspects Determining the Pharmacokinetic Properties of Drugs, in: The Practice of Medicinal Chemistry (Third Edition), 2008, pp. 637–654, doi:10.1016/B978-0-12-374194-3.00031-7.
[69] F. Ntie-Kang, L.L. Lifongo, J.A. Mbah, L.C.O. Owono, E. Megnassan, L.M. Mbaze, P.N. Judson, W. Sippl, A.M.N. Efange, In silico drug metabolism and pharmacokinetic profiles of natural products from medicinal plants in the Congo basin, In Silico Pharma 1 (12) (2013) 1–11, doi:10.1186/2193-9616-1-12.
[70] A. Daina, O. Michielin, V. Zoete, SwissADME: a Free Web Tool to Evaluate Pharmacokinetics, Drug-Likeness and Medicinal Chemistry Friendliness of Small Molecules, Sci. Rep. 7 (2017) 1–13, doi:10.1038/srep42717.
[71] Z. Liu, S. Wang, M. Hu, Chapter 11 - Oral Absorption Basics: pathways, Physico-chemical and Biological Factors Affecting Absorption. Developing Solid Oral Dosage Forms, Pharma, Ther. Pract. (2009) 265–288, doi:10.1016/B978-0-444-53242-8.00011-4.
[72] H. Yang, W. Xie, X. Xue, K. Yang, J. Ma, W. Liang, Q. Zhao, Z. Zhou, D. Pei, J. Ziebuhr, R. Hilgenfeld, K.Y. Yuen, L. Wong, G. Gao, S. Chen, Z. Chen, D. Ma, M. Bartlam, Z. Rao, Design of Wide-Spectrum Inhibitors Targeting Coronavirus Main Proteases, PLoS Biol 3 (10) (2005) 1–11, doi:10.1371/journal.pbio.0030324.
[73] M.U. Mirza, M. Froeyen, Structural elucidation of SARS-CoV-2 vital proteins: computational methods reveal potential drug candidates against main protease, Nsp12 polymerase and Nsp13 helicase, J. Pharma. Anal. (2020) article in press, doi:10.1016/j.jpha.2020.04.008.
[74] Y. Shimamoto, Y. Hattori, K. Kobayashi, K. Teruya, A. Sanjoh, A. Nakagawa, E. Yamashita, K. Akaj, Fused-ring structure of decahydroisoquinolin as a novel scaffold for SARS 3CL protease inhibitors, Bioorg. & Med. Chem. 23 (4) (2015) 876–890, doi:10.1016/j.bmc.2014.12.028.
[75] M. Wang, R. Cao, L. Zhang, X. Yang, J. Liu, M. Xu, Z. Shi, Z. Hu, W. Zhong, G. Xiao, Remdesivir and chloroquine effectively inhibit the recently emerged novel coronavirus (2019-nCoV) in vitro, Cell Res 30 (2020) 269–271, doi:10.1038/s41422-020-0282-0.
[76] J. Lim, S. Jeon, H.Y. Shin, M.J. Kim, Y.M. Seong, W.J. Lee, K.W. Choe, Y.M. Kang, B. Lee, S.J. Park, Case of the Index Patient Who Caused Tertiary Transmission of Coronavirus Disease 2019 in Korea: the Application of Lopinavir/Ritonavir for the Treatment of COVID-19 Pneumonia Monitored by Quantitative RT-PCR, J. Kor. Med. Sci. 35 (6) (2020) 1–6 e79, doi:10.3346/jkms.2020.35.e79.
[77] M.L. Holshue, C. DeBolt, S. Lindquist, K.H. Lofy, J. Wiesman, H. Bruce, C. Spitters, K. Ericson, S. Wilkerson, A. Tural, G. Diaz, A. Cohn, L. Fox, A. Patel, S.I. Gerber, L. Kim, S. Tong, X. Lu, S. Lindstrom, M.A. Pallansch, W.C. Weldon, H.M. Biggs, T.M. Uyeki, S.K. Pillai, First Case of 2019 Novel Coronavirus in the United States, New Engl. J. Med. 382 (2020) 929–936, doi:10.1056/NEJMoa2001191.
[78] J.E. Lesch, in: "Chapter 3: Prontosil". The first Miracle drugs: How the Sulfa Drugs Transformed Medicine, Oxford University Press, 2007, p. 51. ISBN 978-0-19-518775-5.
[79] E. Török, E. Moran, F. Cooke, in: Oxford Handbook of Infectious Diseases and Microbiology, Oxford University Press, Oxford, 2009, p. 56. ISBN 9780191039621.
[80] O.P. Gupta, K.K. Agarwal, Role of Phenazopyridine in Urinary Tract Infections, Ind. J. Clin. Pract. 22 (9) (2012) 437–441.
[81] L.G. Ferreira, R.N. dos Santos, G. Oliva, A.D. Andricopulo, Molecular Docking and Structure-Based Drug Design Strategies, Molecules 20 (2015) 13384–13421, doi:10.3390/molecules200713384.
[82] C.-.W. Lin, C.-.H. Tsai, F.-.J. Tsai, P.-.J. Chen, C.-.C. Lai, L. Wan, H.-.H. Chiu, K.-.H. Lin, Characterization of Trans- and Cis-Cleavage Activity of the SARS Coronavirus 3CLpro Protease: basis for the in Vitro Screening of anti-SARS Drugs, FEBS Lett. 574 (2004) 131–137, doi:10.1016/j.febslet.2004.08.017.
[83] F.S. Hosseini, M. Amanlou, Simeprevir, Potential Candidate to Repurpose for Coronavirus Infection: virtual Screening and Molecular Docking Study. Preprints, (2020), 1–12. doi: 10.20944/preprints202002.0438.v1.
[84] D.C. Hall, H.F. Ji, A search for medications to treat COVID-19 via in silico molecular docking models of the SARS-CoV-2 spike glycoprotein and 3CL protease, Tra. Med. Infect. Dis. (2020) 1–3 article in press, doi:10.1016/j.tmaid.2020.101646.
[85] C. Liu, Q. Zhou, Y. Li, L. Garner, S.P. Watkins, L.J. Carter, J. Smoot, A.C. Gregg, A.D. Daniels, S. Jervey, D. Albaiu, Research and Development on Therapeutic Agents and Vaccines for COVID-19 and Related Human Coronavirus Diseases, ACS Cent. Sci. 6 (2020) 315–331, doi:10.1021/acscentsci.0c00272.
[86] A.I. Owis, M.S. El-Hawary, D. El Amir, O.M. Aly, U.R. Abdelmohsen, M.S. Kamel, Molecular docking reveals the potential of Salvadora persica flavonoids to inhibit COVID-19 virus main protease, RSC Adv 10 (2020) 19570–19575, doi:10.1039/d0ra03582c.
[87] V.S. Sivasankarapillai, A.M. Pillai, A. Rahdar, A.P. Sobha, S.S. Das, A.C. Mitropoulos, M.H. Mokarrar, G.Z. Kyzas, On Facing the SARS-CoV-2 (COVID-19) with Combination of Nanomaterials and Medicine: possible Strategies and First Challenges, Nanomaterials 10 (2020) 1–23 852, doi:10.3390/nano10050852.
[88] S. Khaerunnisa, H. Kurniawan, R. Awaluddin, S. Suhartati, S. Soetjipto, Potential Inhibitor of COVID-19 Main Protease (Mpro) From Several Medicinal Plant Compounds by Molecular Docking Study. Preprints, (2020), 1–14. doi: 10.20944/preprints202003.